Magnetic levitation, suspension, and superconductivity: Macroscopic and mesoscopic

Stephen B. Haley and Herman J. Fink
Department of Electrical and Computer Engineering, University of California, Davis, California, 95616
(Received 3 March 1995; revised manuscript received 12 October 1995)

The levitation state of a large magnetic sphere held in equilibrium above a thick superconducting layer in the Meissner state is a single temperature-independent state as long as the maximum magnetic field at the superconducting (SC) surface does not exceed the critical field $H_c(T)$. In contrast, a magnetic microsphere trapped by a superconducting microring exhibits very different behavior. When the radius b of the SC ring is of the same order as the Ginzburg-Landau coherence length $\xi(T)$, the system exhibits, in general, a small set of distinct, quantized, temperature-dependent levitation and suspension states. For certain discrete values of b the flux in the ring is quantized, and the levitation and suspension heights are temperature independent. An abrupt temperature induced transition in the suspension height is also found for a special set of parameters.

I. INTRODUCTION

It has been known for a long time, from experimentation, that a macroscopic magnet can be repulsively levitated above a type-I superconductor in the Meissner state. Since the discovery of high-temperature type-II oxide superconductors both repulsive levitation, based on partial flux exclusion and flux pinning, and attractive levitation (suspension) based on flux pinning, have been observed in dramatic, popular demonstrations. A very recent review of levitation phenomena and their practical applications is given by Moon.[1] Typically, researchers use magnetic image methods to simulate a superconducting layer that is thick compared with the penetration depth of the magnetic field.[2–4]

Here we study the equilibrium levitation states of a macroscopic and a microscopic magnet-superconducting system. Our investigation is based on electromagnetics coupled with the Ginzburg-Landau theory of superconductivity which includes material properties of the superconductor. Due to fluxoid quantization in a multiply connected superconductor, such as a ring circuit, quantization effects appear in the levitation states when magnetic flux penetrates the space surrounded by a superconductor. In Sec. II we investigate the states of a macroscopic, uniformly magnetized sphere levitated above a singly connected thick superconductor with the magnetic moment oriented at an arbitrary angle to the surface of the superconductor. Since there is a problem with double counting in the literature, we couple the the image method with a direct calculation of the force on the superconductor and compare the result with the variation of the dipole-dipole interaction energy to clarify the source of an error by a factor of 2. In Sec. III the Ginzburg-Landau free energy of a superconducting (SC) microring circuit in the presence of a very small magnetic sphere in a gravitational field is minimized, subject to single valuedness of the complex superconducting order parameter and mechanical equilibrium. The resulting quantized levitation and suspension states, some of which have been reported by Haley,[5] are investigated in detail, and several interesting results are given here. Section IV is devoted to our conclusions.

II. MACROSCROPIC MAGNETIC SPHERE LEVITATED BY A THICK SUPERCONDUCTING SLAB

When a magnet is lowered toward the surface of a thick superconductor, persistent currents in the superconductor are established which produce a magnetic field opposing that of the magnet. The magnet depicted in Fig. 1(a) is a uniformly magnetized sphere with saturation magnetization M_s, radius a, and density ρ. The magnetic moment of the magnet is $M_0 = M_s 4\pi a^3/3$, and the weight $W = (4\pi a^3/3)\rho g$, where g is the gravitational acceleration constant 9.8 m/s^2. A magnetic dipole can be simulated by a current loop of radius a, carrying a fictitious constant current $I_a = M_0/(\pi a^2)$. When the "magnet current" and the current in the superconductor flow in opposite directions, the current loops repel; otherwise they attract. Equilibrium for levitation is achieved when the magnetic force of repulsion equals the weight of the magnet. It is assumed that the superconductor is mounted on a substrate which is fixed. For lateral stability one should make the superconductor surface slightly concave, but this is not considered in our calculations. If the magnetic moment is reversed, the persistent current also reverses, maintaining the levitation state. Assuming the superconductor is much thicker than $\lambda(t)$, the temperature-dependent penetration depth, and the levitation height $h \gg \lambda(t)$, we simulate repulsion by an image magnet, located a distance h below the superconducting surface, as depicted in Fig. 1(b). The variable $t = T/T_c$, with T the temperature, and T_c the critical temperature of the SC–normal phase transition in zero magnetic field.

The magnetic-field components in the (xy) plane due to the magnet shown in Fig. 1(a) are

$$H_x = \frac{3M_0}{4\pi r^5}[xy\ \cos\alpha - hx\ \sin\alpha] \tag{2.1}$$

$$H_y = \frac{3M_0}{4\pi r^5}\left[\left(y^2 - \frac{1}{3}r^2\right)\cos\alpha - hy\ \sin\alpha\right], \tag{2.2}$$

where $r^2 = x^2 + y^2 + h^2$, and α is the tilt angle shown in Fig. 1(b). The total surface field due to the magnet and its image, shown in Fig. 1(b), is then

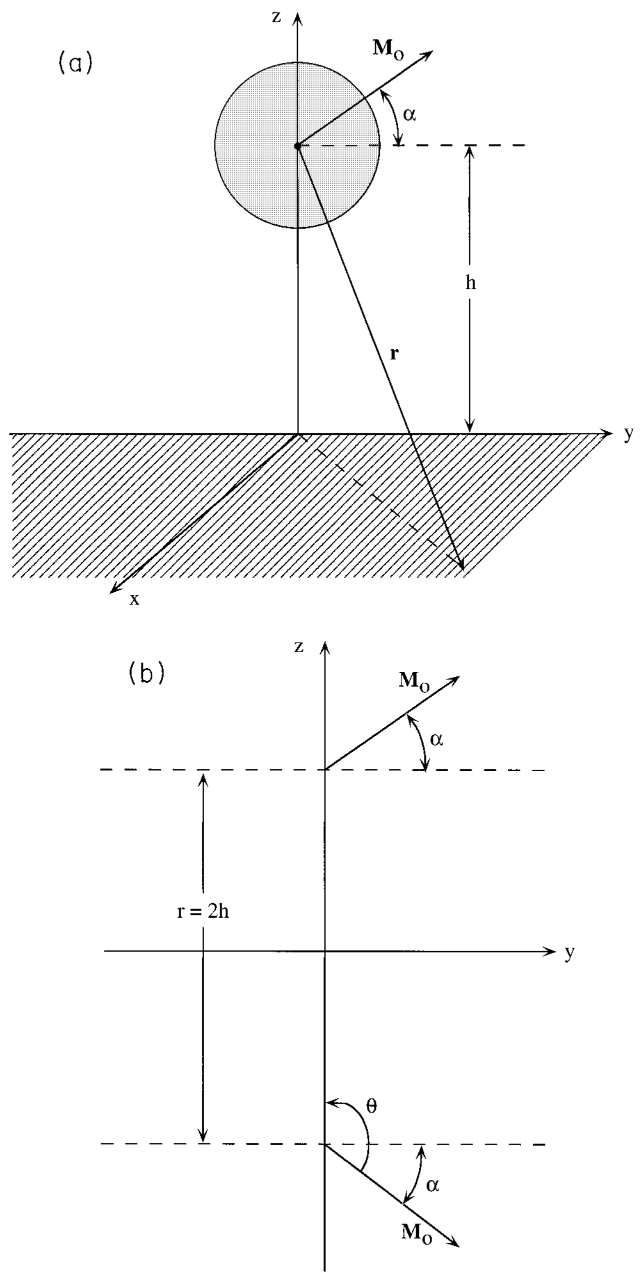

FIG. 1. (a) A magnetic source, modeled by a uniformly magnetized sphere of radius a and moment $\mathbf{M_0}$ at tilt angle α is levitated at height h above a thick superconducting slab. (b) The magnet moment and its image, located at distance h below the SC surface, are shown.

$$\mathbf{H_s}=2\mathbf{H_a}=2(\hat{x}H_x+\hat{y}H_y), \tag{2.3}$$

where $\mathbf{H_a}$ is the applied horizontal component due to the real, source magnet by itself. Treating the superconductor as an ideal conductor, with $\hat{z}$ a unit vector perpendicular to the surface, the sheet current density $\mathbf{K}$ (A/m) is given by

$$\mathbf{K}=\hat{z}\times\mathbf{H_s}=2(-\hat{x}H_y+\hat{y}H_x). \tag{2.4}$$

The sheet current density $\mathbf{K}$ flows in a layer of thickness $\lambda(t)$ at the surface. Since $\lambda(t)\ll h$ we treat $\mathbf{K}$ as a surface current, which gives rise to the Meissner effect.

The induced surface current density $\mathbf{K}(x,y,\alpha)$ is quite complex, and it is didactic to examine it graphiacally. The normalized current density $\mathbf{k}=2\pi h^3\mathbf{K}/(3M_0)$, which is a function only of the normalized coordinates $x'=x/h$, $y'=y/h$, and the tilt angle α defined in Fig. 1, is plotted in Figs. 2(a)–2(c). The surface $k(x',y')$ is shown with a cutout to view the contours of constant k projected on the (x',y') plane. In Fig. 2(a) the tilt angle α is 90°, and k exhibits cylindrical symmetry, with a minimum of value zero at the origin, and a maximum of value $k_m=0.286$ at $\rho'=0.5$. The current follows the contours, flowing clockwise. Decreasing α breaks the symmetry, as seen in Fig. 2(b), with $\alpha=45°$, and Fig. 2(c), with $\alpha=0°$. The current flow for $\alpha=0$ is depicted by the vector field $\mathbf{k}(x',y')$ plotted in Fig. 2(d), which shows a clockwise vortex and an antivortex corresponding to the local minima of k plotted in Fig. 2(a). In contrast with Fig. 2(a), the current $\mathbf{k}$ does not follow the contours in Fig. 2(c). The contrast is most apparent on the x axis, where the current flow is parallel to the axis, but the contour of constant k is perpendicular.

The force on the magnet, which is opposite to that on the superconductor, is

$$\mathbf{F}=-\mu_0\int_{-\infty}^{\infty}\int_{-\infty}^{\infty}dx\ dy\ \mathbf{K}\times\mathbf{H_a}$$
$$=\hat{z}8\mu_0\int_0^{\infty}\int_0^{\infty}dx\ dy(H_x^2+H_y^2). \tag{2.5}$$

Note that the applied (external) field $\mathbf{H_a}$ acting on the current $\mathbf{K}$ produces the force and not the total surface field $\mathbf{H_s}$. Using Eqs. (2.1) and (2.2), Eq. (2.5) leads to

$$F_z=\frac{3\mu_0M_0^2}{64\pi h^4}(1+\sin^2\alpha). \tag{2.6}$$

Equation (2.6) is by a factor of 2 smaller than equations given by Yang *et al.*[4] and Hellman *et al.*,[3] but it follows from the general equation [2-(2.4)] by Moon.[1] The equilibrium levitation height is obtained from Eq. (2.6) by setting $F_z=W$, which yields

$$h=\frac{\sqrt{M_0}}{2}\left[\frac{3\mu_0(1+\sin^2\alpha)}{4\pi W}\right]^{1/4}. \tag{2.7}$$

For $\alpha=90°$, for example, assume the sphere is iron with $M_s=1.74\times10^6$ A/m, $\rho=7.85\times10^3$ kg/m^3. For a radius $a=0.25$ cm, the magnetic moment $M_0=0.114$ A m^2, the weight $W=5.04\times10^{-3}$ N, and the resulting levitation height is $h=1.8$ cm. The height is temperature independent since M_0 is essentially constant well below the Curie temperature. At first sight Eq. (2.7) seems to be independent of the superconductor. However, the magnetic field anywhere at the SC surface should not exceed the thermodynamic critical field

$$H_c(t)=\frac{\phi_0}{2\sqrt{2}\pi\mu_0\lambda(t)\xi(t)}=H_c(0)(1-t^2), \tag{2.8}$$

where $\phi_0=h/(2|e|)=2.07\times10^{-15}$ Weber is the fluxoid quantum, and $\xi(t)$ is the Ginzburg-Landau coherence length. Equating the maximum of H_s in Eq. (2.3) to

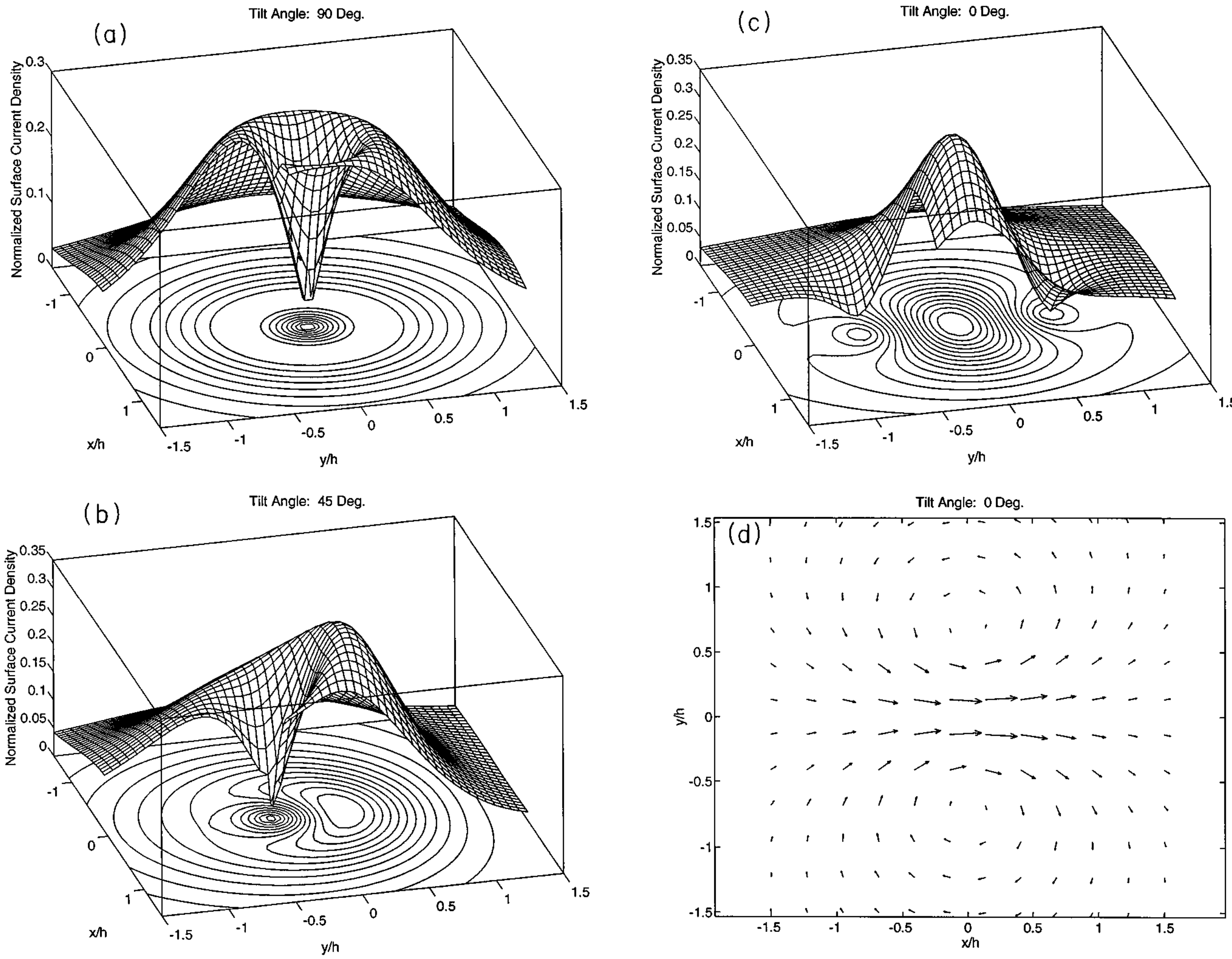

FIG. 2. The normalized, unitless surface current density magnitude k is shown as a surface $k(x/h, y/h)$ with contours of constant k for (a) $\alpha=90°$, (b) $\alpha=45°$, (c) $\alpha=0°$. The vector field $\mathbf{k}(x/h, y/h)$ is plotted in (d) for $\alpha=0°$.

$H_c(0)(1-t_m^2)$, with $H_c(0)=6.4\times10^4$ A/m for lead, gives $t_m=0.987$. Above $t=t_m$, the height h decreases to zero.

The result (2.7) can also be obtained from energy considerations. The magnetic energy arising from the real magnetic moment in the field of the image magnet is

$$U=-\mathbf{M_0}\cdot\mathbf{B}. \tag{2.9}$$

In spherical coordinates, with $\theta=90°+\alpha$, and $\mathbf{r}=2h\hat{z}$ the distance from the image to the source magnet, the magnetic-flux density and moment are

$$\mathbf{B}=\frac{\mu_0 M_0}{4\pi r^3}(\hat{r}2\cos\theta+\hat{\theta}\sin\theta), \quad \mathbf{M}_0=M_0(\hat{r}\sin\alpha-\hat{\theta}\cos\alpha).$$

Using the above, the energy U reduces to

$$U=\frac{\mu_0 M_0^2}{4\pi r^3}(1+\sin^2\alpha). \tag{2.10}$$

The force $F_z=-(\partial U/\partial r)_{r=2h}$ reproduces Eq. (2.6), from which follows the equilibrium levitation height, Eq. (2.7).

Based on the lower energy with $\alpha=0$, we conjecture that the moment parallel to the surface is the preferred configuration, as observed experimentally for a bar magnet (see Shoenberg,[6] p. 20). The moment and weight dependences of Eq. (2.7) are different than those obtained by Orlando and Delin[7] for a magnetic disk using a uniform magnetic-field approximation which is a poor approximation for a spherical magnet.

III. LEVITATION AND SUSPENSION OF A SMALL MAGNETIC PARTICLE BY A SUPERCONDUCTING MICRORING

The spherical magnet shown in Fig. 3(a) is levitated above a superconducting microring of radius b and wire cross-sectional area s mounted on a fixed insulating substrate. The value of h is positive for levitation and negative for suspension. The magnet is uniformly magnetized with magnetic moment $\mathbf{M}=M_0\hat{z}$, and the weight is W, as in Sec. II. The SC ring carries an induced current I, and has self-inductance L. The SC ring material is characterized by the temperature-dependent magnetic-field penetration depth $\lambda(t)$ and the Ginzburg-Landau (GL) coherence length $\xi(t)$.

The height h is determined self-consistently by minimizing the total free energy of the system consisting of the magnet and SC ring, subject to fluxoid quantization and mechani-

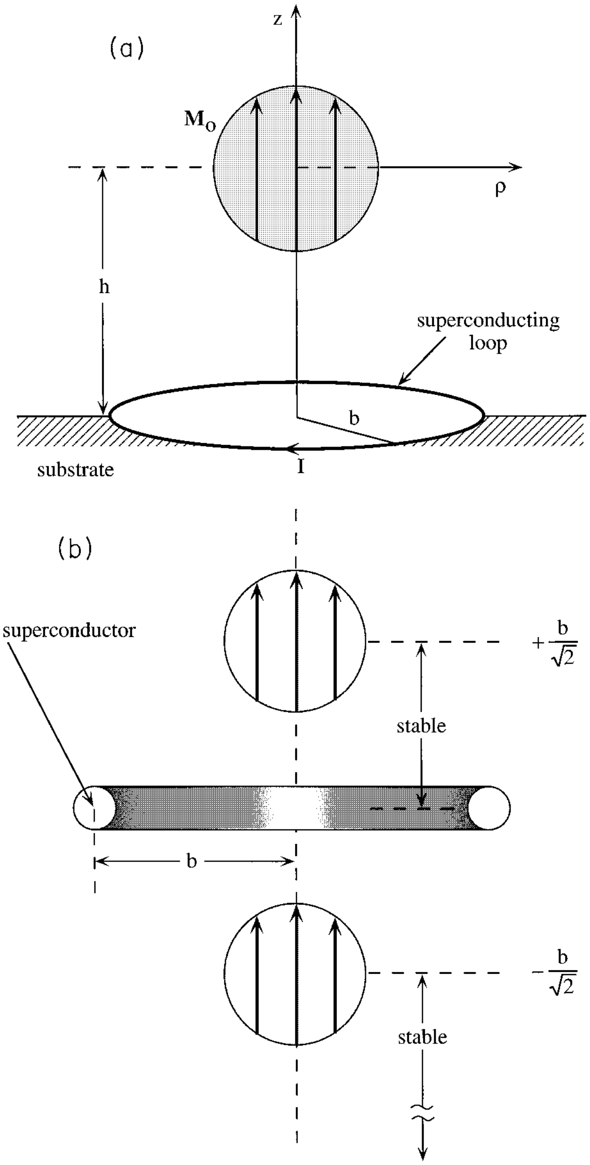

FIG. 3. (a) The magnetic sphere of radius a is levitated by a superconducting ring of radius b and wire cross section s, carrying an induced current I. The levitation height is h. (b) Side view showing the regions of stability to horizontal displacement.

cal equilibrium constraints. Since the magnetic field at the SC ring is not a controllable external variable, the Helmholtz free energy F is the appropriate functional to be minimized.[8] The difference between the SC and normal-state free energies is

$$\Delta F = \frac{\Lambda(t)}{V_s}\int dv\left[-N+\frac{1}{2}N^2+NQ^2+(\xi\nabla\sqrt{N})^2\right]+\frac{1}{2}LI^2 + \phi_a I + Wh, \tag{3.1}$$

where $\Lambda(t)=\mu_0 V_s H_c^2(t)$, with V_s the volume of the SC ring and $H_c(t)$ is the thermodynamic critical magnetic field. The first two terms in the integrand are the normalized condensation energy of the superconductor, with $N=|\psi|^2$, where $\psi=\Psi/\Psi_{\text{bulk}}=\sqrt{N}\exp(i\theta)$ is the normalized complex order parameter. The last two terms comprise the kinetic energy $K=\xi^2|\mathbf{p}\psi|^2$, where $\mathbf{p}=-i\nabla+(2\pi/\phi_0)\mathbf{A}$, with $\mathbf{A}$ the magnetic vector potential. The magnetic energy term $0.5LI^2$ is not constant, since the SC current I varies with the magnet height. The flux coupling energy between the magnet and the superconductor is $\phi_a I$, with ϕ_a the "applied" magnetic flux enclosed by the SC ring due to M_0. If one models the magnetic dipole by a ring circuit of radius a, carrying a fictitious constant current $I_a=M_0/(\pi a^2)$, the coupling energy term may be written as $I_a MI$, where M is the mutual inductance. This term is positive if I_a and I flow in *opposite* directions, but negative if they flow in the same direction. Note that $0.5LI^2+\phi_a I$ comprise the height-dependent parts of the total energy stored in the magnetic fields of the ring coupled to the magnet. The last term, Wh, is the gravitational potential energy of the magnet with respect to the plane of the SC ring.

The normalized quantum current density is defined by

$$\mathbf{J}_\psi = \xi\ \text{Re}(\psi^*\mathbf{p}\psi)=N\mathbf{Q}, \tag{3.2}$$

where $\mathbf{Q}=\xi[\nabla\theta+(2\pi/\phi_0)\mathbf{A}]$ is usually called the normalized superfluid velocity. It should be noted that I in (3.1) and the current I_ψ are not necessarily the same. The definition of the latter is linked to the Gibbs free energy G. One of the equations obtained from the first variation of G is $\nabla\times\nabla\times\mathbf{Q}-\nabla\times\mathbf{H}_a+N\mathbf{Q}=0$ with the above defined $\mathbf{Q}$. Only if the applied magnetic field H_a is curl free (which applies to our case) and $\nabla\times\nabla\times\mathbf{Q}$ is replaced by $-J$ does one obtain $J=J_\psi$, where J_ψ is defined by (3.2). Taking a contour integral of $\mathbf{Q}$ around the SC ring, requiring single-valuedness of the complex order parameter, gives the flux quantization constraint

$$\oint \mathbf{dl}\cdot\mathbf{Q}=2\pi\xi\left(\frac{\phi}{\phi_0}+n\right), \tag{3.3}$$

where the phase winding number n is an integer or zero, and ϕ is the total flux enclosed by the contour. Explicitly

$$\phi=\phi_a - LI. \tag{3.4}$$

The SC current I, in Eq. (3.4), is positive for levitation and negative for suspension, whereas ϕ_a is always positive.

The gravitational force and the interaction of the SC ring with the magnet produces a net force on the magnet given by

$$\mathbf{F}=\mu_0\int dv\, j(\hat{\rho}H_z-\hat{z}H_\rho)-\hat{z}W, \tag{3.5}$$

where j is the SC current density, and H_z and H_ρ are the components of the field due to the magnet, evaluated at the SC ring. In a stable equilibrium state the force $\mathbf{F}=0$. Since the net horizontal force component must be zero, the superconductor must generate a restoring force that constrains the magnet to the axis of symmetry of the ring. Stability is discussed below. For now, assume the magnet remains as depicted in Fig. 3(a).

For the uniformly magnetized sphere, depicted in Fig. 3(a), the magnetic vector potential, in cylindrical coordinates with the origin at the center of the magnet, is

$$\mathbf{A}_a(\rho,z)=\hat{\phi}\frac{\mu_0 M_0}{4\pi}\frac{\rho}{(\rho^2+z^2)^{3/2}}.$$

The applied flux ϕ_a at the ring, calculated from the line integral of $\mathbf{A}_a(b,-h)$, is

$$\phi_a=\frac{\mu_0 M_0}{2b}\frac{1}{(1+x^2)^{3/2}}, \tag{3.6}$$

with normalized height $x=h/b$. The field components are determined from $\mu_0\mathbf{H}=\nabla\times\mathbf{A}_a$. In cylindrical coordinates, the ρ component of the magnetic field at the superconducting ring, and the z component anywhere in the plane of the ring are

$$H_\rho=-\frac{3M_0}{4\pi b^3}\frac{x}{(1+x^2)^{5/2}}, \quad H_z=\frac{M_0}{4\pi b^3}\frac{2x^2-(\rho/b)^2}{(1+x^2)^{5/2}}. \tag{3.7}$$

The wire cross section s is assumed small so that the transverse variations of $N,\mathbf{Q}$, and $\mathbf{H}$ in the SC ring are small. In this limit, the integrals in Eqs. (3.1), (3.3), and (3.5) may be replaced by their mean values. The fluxoid quantization constraint Eq. (3.3) then yields

$$Q=\frac{\xi}{b}\left(\frac{\phi}{\phi_0}+n\right), \tag{3.8}$$

where Q is now a measure of the normalized flux enclosed by the ring relative to a quantum number. Equation (3.8) links the mean value of Q to the current I via Eq. (3.4). Q, I, and ϕ_a are explicit functions of height h and therefore our independent variables in the free energy are N and h. In the same approximation, Eq. (3.5), noting that $\phi_a'=2\pi\mu_0 bH_\rho$, gives the vertical components of $\mathbf{F}$ and $\partial\mathbf{F}/\partial h$ as

$$F_z=-I\phi_a'-W, \tag{3.9a}$$

$$F_z'=-I'\phi_a'-I\phi_a''. \tag{3.9b}$$

The primes denote partial derivatives with respect to h. At equilibrium $F_z=0$, and $F_z'=0$ as discussed after Eq. (3.13). Consistent with our thin wire approximation and the cylindrical symmetry of the system, we neglect the integral of $(\xi\nabla\sqrt{N})^2$ in Eq. (3.1). Defining a normalized energy $E=\Delta F/\Lambda(0)$, it follows from Eq. (3.1) that

$$E=E_{\rm sc}(t)+\frac{1}{\Lambda(0)}\left[\frac{1}{2}LI^2+\phi_a I+Wh\right], \tag{3.10}$$

where the explicit SC contribution is

$$E_{\rm sc}(t)=\left(-N+\frac{1}{2}N^2+NQ^2\right)(1-t^2)^2.$$

Before considering the general problem of minimizing E, subject to equilibrium constraints, it is elucidating to examine the parts. The term $E_{\rm sc}$ is minimum for $N=1$ and $Q=0$. In a levitation state, $(I>0,\ x>0)$, the second term in Eq. (3.10) is always positive; thus the free energy E is an absolute minimum when $N=1$, $Q=0$, and the bracket is minimized. At equilibrium, using Eq. (3.9a) with $F_z=0$, the bracket in Eq. (3.10) is minimum with respect to variation in h when

$$I'=0, \tag{3.11a}$$

or

$$-\frac{WL}{\phi_a'}+\phi_a=0. \tag{3.11b}$$

Noting that $I=-W/\phi_a'$, Eq. (3.11b) is satified only for a suspension state, $(I<0,\ x<0)$. To acheive an absolute minimum energy for a levitation state Eq. (3.11a) must hold, and Eq. (3.9b) requires that $F_z'=-I\phi_a''$ at equilibrium.

The normalized free energy E, Eq. (3.10), is a function of the N and h. Minimizing E with respect to variation in N gives

$$N=1-Q^2, \tag{3.12}$$

which satisfies the absolute miniumum energy condition $N=1$ and $Q=0$. We note that, in general, the variation of $\Delta F(N,Q,I,h)$ with respect to $N(\mathbf{r})$ yields the GL equation $\xi^2\nabla^2\sqrt{N}=\sqrt{N}(N-1+Q^2)$. Thus, neglecting the $\nabla^2\sqrt{N}$ term gives a point variable form identical to Eq. (3.12).

The variation of E with respect to h, using Eqs. (3.8) and (3.9a) with $F_z=0$, leads to the relation

$$\frac{\beta}{(\phi_a')^2}\left[\frac{WL-\phi_a\phi_a'}{1-L(I'/\phi_a')}\right]I'=NQ, \tag{3.13}$$

where $\beta=\lambda(t)/[\sqrt{2}sH_c(t)]$. It is seen that when $Q=0$ (when the flux through the ring is quantized), Eq. (3.13) requires that Eqs. (3.11a) or (3.11b) hold at equilibrium. Equation (3.11b) is a well defined function of h, but the only relation involving I' is Eq. (3.9b) in which F_z', is the coefficient of the linear term in an expansion of F_z about the equilibrium value. For $Q=0$, the levitation solutions that minimize E require that $I'=0$, and thus from Eq. (3.9b) that $F_z'=-I\phi_a''$. The absolute minimum value of E occurs when $x=0.5$, at which point $\phi_a''=0$, and thus $F_z'=0$. The corresponding $Q=0$ suspension solutions that minimize E satisfy Eq. (3.11b), and are independent of I' and hence F_z'. In light of these results we expect the lowest-energy solutions will have $Q\ll 1$. Since the minimum value of E is independent of F_z' for any value of Q, Eq. (3.13) must also be independent of F_z'. Consistency requires that $F_z'=0$, which is an interesting result: The leading term in the restoring force is not linear in the displacement from equilibrium. Setting $F_z'=0$ gives $I'=-I\phi_a''/\phi_a'$, and Eq. (3.13) using Eq. (3.12) assumes the form

$$J=(1-Q^2)Q/(1-\Omega). \tag{3.14}$$

The height-dependent variable Ω is defined by

$$\Omega(h)=\frac{1-\phi_a\phi_a''/(\phi_a')^2}{1-WL[\phi_a''/(\phi_a')^3]}. \tag{3.15}$$

The normalized SC current density is $J=\beta I$. The variables J and Q in Eq. (3.14) are interpreted as mean values taken over the volume of the SC ring. Equation (3.14) shows that J is not equal to the quantum-mechanical expression J_ψ and that the effective electron pair velocity is $Q/(1-\Omega)$ in our case. Thus, when $Q\to 0$, the variable $\Omega\to 1$ for a finite levitation or suspension current. Neglecting Ω is equivalent to starting with a free energy without the mutual inductance term $\phi_a I$.

Using the fluxoid quantization equation (3.8) and Eq. (3.9a) with $F_z=0$, Eq. (3.14) gives the equilibrium height equation

$$y(x)\equiv\left(\frac{\phi}{\phi_0}+n\right)^3-\left(\frac{b}{\xi}\right)^2\left(\frac{\phi}{\phi_0}+n\right)+C\left(\frac{1-\Omega}{\phi_a'}\right)=0, \tag{3.16}$$

with the constant C defined by

$$C=\frac{2\pi\mu_0 bW}{\phi_0}\frac{(\kappa b)^2}{s},$$

where $\kappa=\lambda/\xi$. The total flux, using Eqs. (3.4) and (3.9a), is

$$\phi=\phi_a+\frac{WL}{\phi_a'}. \tag{3.17}$$

Equation (3.16), using Eq. (3.17), is a self-consistent equation for the temperature-dependent normalized height $x(t,n)=h(t,n)/b$ of the levitated (or suspended) magnet.

Before investigating the general temperature-dependent solutions of Eq. (3.16), we analyse the important special cases arising from exact flux quantization. When $Q=0$ it follows from Eq. (3.14) that $\Omega=1$. Since t appears only as a coefficient of the flux in Eq. (3.16), it is satisfied for any value of $\xi(t)$ when $Q=0$ and $\Omega=1$. [Note that in accordance with Eq. (3.9a) at equilibrium J cannot be zero.] Thus magnet height h is temperature independent when the total flux is quantized. For $Q=0$, Eq. (3.8) using Eq. (3.17) gives

$$\phi_a+\frac{WL}{\phi_a'}+n\phi_0=0. \tag{3.18}$$

The condition $\Omega=1$ is satisfied if and only if

$$\phi_a''=0, \tag{3.19a}$$

or

$$\phi_a=\frac{WL}{\phi_a'}. \tag{3.19b}$$

Condition (3.19a) is satisfied for $x=\pm 0.5$. In this case Eq. (3.18) determines the radius b of the SC ring for a given phase winding number n. The condition (3.19b) requires that $x<0$, i.e., suspension, and that the induced flux equal the ''applied'' flux. Substituting Eq. (3.19b) into Eq. (3.18) gives the half-flux quantum condition for suspension

$$\phi_a=-\frac{n}{2}\phi_0. \tag{3.20}$$

Together, Eqs. (3.20) and (3.19b) determine b and x for a given n.

To further understand the significance of the quantized flux solutions, let us examine the energy E in more detail. Using Eqs. (3.6), (3.9a), and (3.12), at mechanical equilibrium one obtains

$$E=-\frac{1}{2}(1-Q^2)^2(1-t^2)^2 + \frac{W}{6\pi\mu_0 sH_c(0)^2}\left[\frac{2b^3WL}{3(\mu_0M_0)^2}\frac{(1+x^2)^5}{x^2}+\left(\frac{1}{x}+4x\right)\right]. \tag{3.21}$$

The first term in Eq. (3.21) is the normalized energy of the SC ring, which is minimum when $Q=0$. The term $(1/x+4x)$ arises from $\phi_a I+Wh$ and the other from the self-inductance. For $x>0$ all terms are positive, and the bracket has an absolute minimum for $x=0.5$. Therefore, when $Q=0$, the energy E assumes its absolute minimum value for levitation at height $h=0.5b$, consistent with Eq. (3.19a).

All calculations and figures are based on the following data: The magnetic particle is an yttrium iron garnet (YIG) sphere of radius $a=0.4$ μm, saturation magnetization $M_s=2\times10^5$ A/m and density $\rho=5.2\times10^3$ kg/m^3, with resultant magnetic moment $M_0=5.36\times10^{-14}$ A m^2, and weight $W=1.37\times10^{-14}$ N. The SC ring has wire cross section $s=10^{-14}$ m^2 and various radii b. The SC ring is Al with zero-temperature values of the penetration depth and coherence length taken as $\lambda(0)=0.05$ μm and $\xi(0)=\xi_0=1.6$ μm.[9] The temperature dependence used is $\lambda(t)=\lambda(0)/\sqrt{1-t^2}$ and $\xi(t)=\xi(0)/\sqrt{1-t^2}$; thus $\kappa=\lambda/\xi$ is temperature independent. The critical field for Al is $H_c(0)=0.79\times10^4$ A/m, and the critical current in the ring at $t=0$ is $I_c=(2/\sqrt{27})[\sqrt{2}sH_c(0)]/\lambda(0)=0.97$ mA. The self-inductance of the ring is

$$L\approx\mu_0 b\left[\ln\left(\frac{8b}{\sqrt{s/\pi}}\right)-1.75\right].$$

The temperature-independent, absolute minimum energy, levitation solutions require $Q=0$ and $x=0.5$. They are determined by Eq. (3.18), which reads

$$\frac{\mu_0M_0}{2b(1+x^2)^{3/2}}\left[1-\frac{4WLb^3}{3(\mu_0M_0)^2}\frac{(1+x^2)^4}{x}\right]=-n\phi_0. \tag{3.22}$$

With $x=0.5$ Eq. (3.22) yields the ordered pairs

$[n,\ b_n(\mu\mathrm{m})]$: . . . [0, 9.30], . . . [−3, 3.80],[−4, 2.89], . . .

[−9, 1.30] . . . .

These discrete radii correspond to levitation height $h=0.5b$, which is temperature independent until the current in the ring exceeds the critical current of the superconductor. Of course levitation occurs only if I is smaller than the critical current at absolute zero, namely $I_c=0.97$ mA. If a particular b_m is used in the general equation (3.16), only solutions for $n\geq m$ are physical $(1\geq N>0)$, and those with $n>m$ are weakly temperature dependent.

The temperature-independent suspension solutions are determined from the coupled Eqs. (3.19b) and (3.20), explicitly given by

$$\frac{3(\mu_0M_0)^2}{4W}=-b^3L\frac{(1+x^2)^4}{x} \tag{3.23}$$

and

$$\frac{\mu_0 M_0}{\phi_0} = -nb(1+x^2)^{3/2}. \tag{3.24}$$

With the phase winding number n and all magnet properties fixed, assuming that the wire cross section s is known, Eqs. (3.23) and (3.24) can be solved uniquely for b and x. Alternatively, if one were to fix b and leave n and x as the two unknowns, then Eqs. (3.23) and (3.24) cannot be satisfied *in general* with n an integer. Equation (3.24) restricts n to negative values. For our data, the ordered triplets which solve Eqs. (3.23) and (3.24) are

$$[n,\ b(\mu\text{m}),\ x]:[-1, 4.19, -1.71],[-2, 8.23, -0.759],$$
$$[-3, 9.42, -0.316].$$

There are no other solutions.

Stability of the magnet to horizontal displacement is determined by the ρ component of Eq. (3.5). Domains in which there exists a self-centering, horizontal restoring force are shown in Fig. 3(b). As pointed out in Ref. 5 for $0<x<1/\sqrt{2}$ the levitation solutions with $I>0$ are stable, whereas suspension solutions with I reversed are stable for $x<-1/\sqrt{2}$. Thus all of the above absolute minimum energy, quantized flux, levitation solutions with $x=0.5$, and the quantized flux suspension solutions for $n=-1$ and $n=-2$ are stable; whereas the $n=-3$ suspension solution is not stable, nor is the $x=-0.5$ solution which satisfies Eq. (3.19a). When $\Omega=0$ the equilibrium current density $j=-W/(s\phi_a')$ equals the quantum-mechanical current density $[\sqrt{2}H_c(t)/\lambda(t)]NQ$. To obtain this condition, Eq. (3.15) requires that $|x|=1$, or $|x|$ infinite. Only the suspension solution at $x(t)=-1$ is stable.

In general, if the total flux in the SC ring is not quantized, i.e., when $\phi\neq -n\phi_0$ which requires that $Q\neq 0$, then the parameter $x=h/b$ is determined by Eq. (3.16). However, since all solutions which relate to the lowest stable energy have a constant and temperature-independent levitation height $h=0.5b$, and a stable levitation height cannot exceed $h=0.707a$, the height of stable levitation states are not strongly temperature dependent and remain close to $0.5b$ as the temperature is varied.

We now turn our attention to the general temperature-dependent solutions of Eq. (3.16). The function $y(x)$ has a root x_0 that corresponds to the minimum value of ΔF. For a given set of parameters, there is a minimum and a maximum value of n for which the root x_0 exists, i.e., $n_{\min}\leqslant n\leqslant n_{\max}$. For each n, as the temperature t increases, x_0 disappears at a cutoff temperature $t=t_{co}\leqslant t_c$.

Figure 4 shows the quantized, normalized levitation height $h(t,n)/b$ plotted as a function of $t=T/T_c$ for SC ring radius $b=3.345$ μm. This radius is the average of the discrete radii corresponding to the $n=-3$ and $n=-4$ quantized flux, temperature-independent solutions. Three levels are shown from the complete set of fluxoid quantum numbers in the range $n_{\min}=-3$ to $n_{\max}=3$ for which levitation solutions exist. Only the $n=-3$ level in the complete set is horizontally stable. As n increases, the levels become increasingly temperature dependent, with a decreasing cutoff temperature t_{co}. For this "intermediate" radius, other parameters, E, J/J_c, and N are plotted in Figs. 5–7. It is seen that the normalized total free energy E, calculated from Eq. (3.10) is dominated by the condensation energy, with $N\approx 1$, for $n=-3$; whereas for $n=3$ energy is extracted from the condensate to lift the magnet to a higher levitation state. For $n=-3$ the normalized current density J exceeds J_c for t slightly less than $t=t_{co}$, but for higher values of n it does not. The behavior of the $n=3$ current density is due to the relatively large value of Q on the right side of Eq. (3.14). The maximum of J occurs at $t=0.29$, at which point $Q=1/\sqrt{3}$ and $J_\psi=J_c=2/\sqrt{27}$. The corresponding value $N=2/3$ also occurs at $t=0.29$ as seen in Fig. 7.

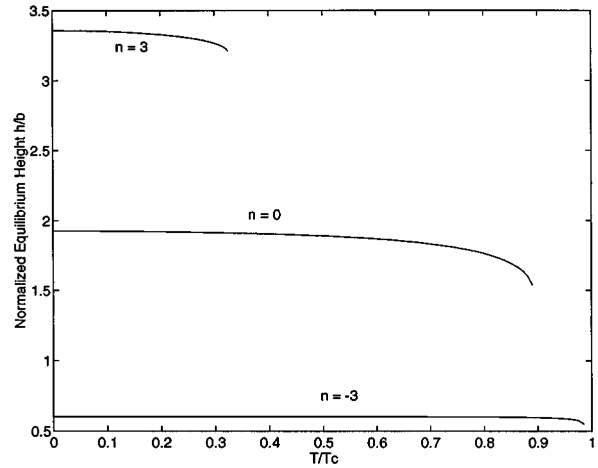

FIG. 4. Quantized, normalized levitation height $h(t,n)/b$ plotted as a function of $t=T/T_c$ for SC ring radius $b=3.345$ μm for three values of the fluxoid quantum number n in the range $n_{\min}=-3$ to $n_{\max}=3$ for which levitation solutions exist. Each curve has a distinct cutoff temperature.

Figure 8 shows the energy E plotted as a function of normalized height h/b at temperature $T=0$ for a SC ring of radius $b=1.295$ μm, at three fluxoid quantum numbers $n=-7,-8,-9$. Total flux is quantized only for the $n=-9$ temperature-independent level. All three states are horizontally stable, and lie in narrow potential wells. The higher, horizontally unstable states have shallow, overlapping energy wells, indicating possible vertical instability.[5]

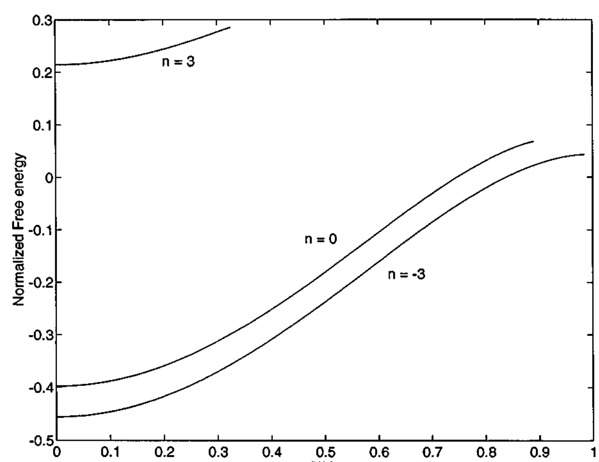

FIG. 5. Normalized free energy E as a function of t. Parameters are the same as in Fig. 4.

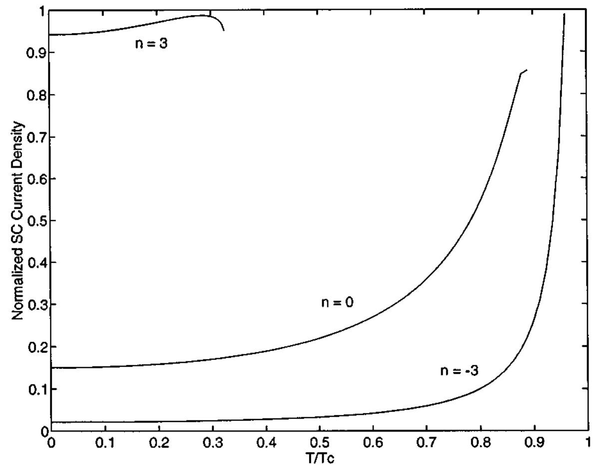

FIG. 6. Normalized SC current density as a function of t. Parameters are the same as in Fig. 4.

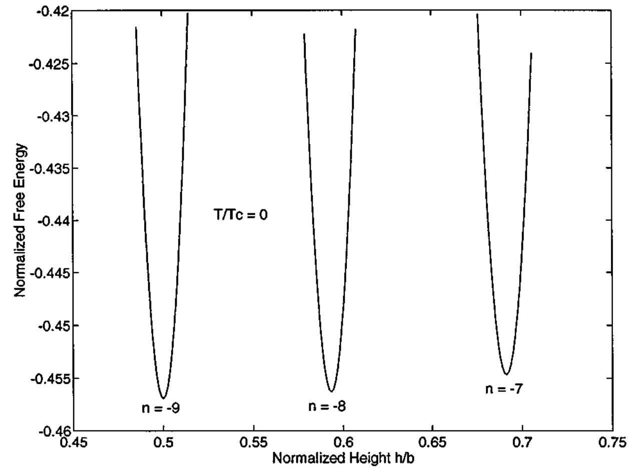

FIG. 8. The normalized total free energy E of the levitation states for fluxoid quantum numbers $n=-7,-8,-9$ are plotted as a function of normalized height h/b at temperature $T=0$ for SC ring radius $b=1.295$ μm. Total flux is quantized for the $n=-9$ level which is temperature independent. All states are horizontally stable.

Figures 9 and 10 show a strong temperature-dependent ''transition'' state for $b=7.28$ μm. For this radius a solution exists only for $n=-2$. The suspension height h/b is plotted as a function of t, in Fig. 9, which shows a rather sharp transition at $t_{\mathrm{tran}}=0.667$ between the unstable and stable regions. The total flux in the ring, plotted in Fig. 10, exhibits similar behavior. Other parameters, not shown, also exhibit unusual behavior. The pair density N has a small, abrupt decrease at t_{tran}; whereas the energy E is a smooth function of t. The normalized current density J, has a small, abrupt increase in magnitude at t_{tran}, with $J<J_c$ for $t<0.85$. The superfluid velocity $Q\ll 1$ for the entire temperature range.

IV. CONCLUSIONS

We have studied the levitation of a macroscopic magnet over a superconducting sheet of thickness much larger than $\lambda(t)$. We find that the magnet with the moment parallel to the sheet has a levitation height which is 84% of the levitation height with the moment perpendicular to the sheet [compare Eq. (2.7) for $\alpha=0$ and $\alpha=\pi/2$]. As long as the sheet is in the Meissner state, with no flux locked in, the magnet is, in principle, unstable to lateral displacement. However, a ''depression'' in the sheet will stabilize the lateral motion (see plate 1 in Shoenberg[6]). When the tangential component of the surface field exceeds $H_c(t)$, the thermodynamic critical field, the levitation height decreases.

Magnetic suspension states, arising from flux pinning in a macroscopic disk of a high-T_c superconductor is a well established phenomenon (see plates 1–10 by Moon[1]). For a mesoscopic SC microring of radius of the coherence length $\xi(t)$ (e.g., $\xi\geqslant 1.6$ μm for Al) and a magnetic sphere of radius in the same range, we find both levitation and suspension states which depend on the fluxoid quantum number. Equation (3.16) determines the levitation and suspension states of a spherical magnet with moment perpendicular to the plane of the SC ring as a function of temperature. Stable levitation states occur in the range $h=0.5b$ to $h=0.707b$. Levitation states above $h=0.707b$ are unstable to lateral displacement [see Fig. 3(b)]. Stable suspension states are possible for

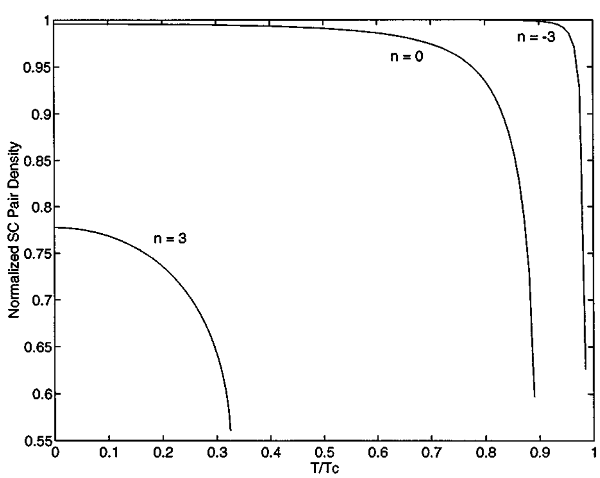

FIG. 7. Normalized SC pair density as a function of t. Parameters are the same as in Fig. 4.

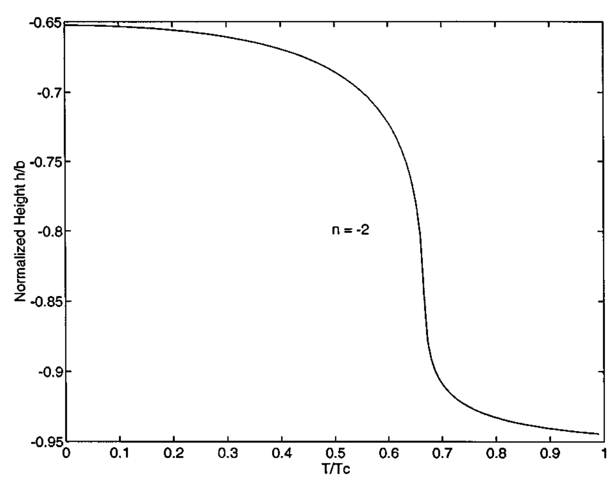

FIG. 9. ''Transition'' state for $b=7.28$ μm. Suspension height h/b versus t, exhibiting a sharp transition at $t_{\mathrm{tran}}=0.667$. A physical solution exists only for $n=-2$.

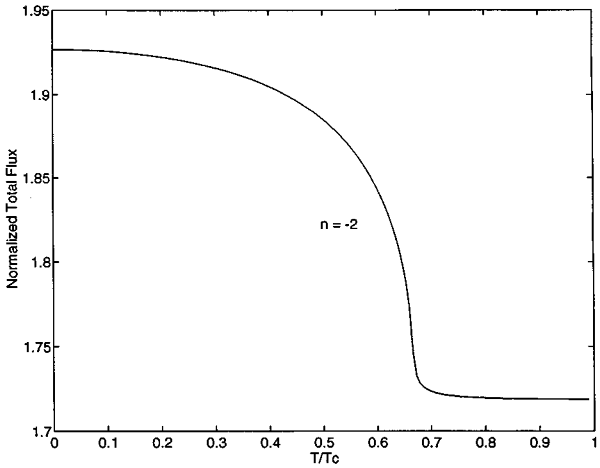

FIG. 10. Transition state: Total flux ϕ linking the ring is plotted versus t.

$h < -0.707b$, and are horizontally unstable for $0 > h > -0.707b$. For certain "quantized" (discrete) radii of the ring, which depend on the fluxoid quantum number n, the levitation height h is one-half the ring radius and temperature independent. This occurs when the flux through the ring is quantized in units of the fluxoid quantum and the average supercurrent velocity Q in the ring is zero. For radii in between the quantized values, Eq. (3.16) leads to slightly temperature-dependent levitation heights. Temperature-independent suspension states are also found. For these states, the distance of the suspended magnet depends both on fluxoid quantum number and ring size. Again, states in-between the temperature-independent suspension distances are slightly temperature dependent for most values of ring radii. For certain radii, we find an abrupt "transition" state in which the suspension distance is strongly temperature dependent.

Comparing the results of Secs. II and III, we find from Eq. (2.4) for a perpendicular moment ($\alpha = \pi/2$) that the largest sheet current density occurs at distance $\rho_m = 0.5h$ from the center of the ring. Thus $h:\rho_m = 2:1$. This compares to $h:b = 1:2$ for the ring current discussed in Sec. III when the flux is exactly quantized. Intuitively this is consistent with the fact that a continuum of current loops flowing parallel to each other will give rise to a larger lift force than a single loop can produce. From Figs. 2(a) and 2(d) it is evident that only the perpendicular moment configuration ($\alpha = \pi/2$) will be supported by a thin ring. In general, when the current in the superconductor exceeds the critical current $I_c(t)$ the magnet falls. Depending on the superconductor, this could happen well below the transition temperature T_c.

Experimental observation of the quantization effects investigated in Sec. III is certainly a challenging problem. The SC ring radius must be in the mesoscopic domain. Using current fabrication technology, only type-I superconductors satisfy the requirements. The suspension states and the lower-lying levitation states are stable, and should be observable in the mesoscopic domain. Recent advances in the development of optical "tweezers" using laser microbeams to trap and manipulate micron-sized biological particles may make it possible to position a magnetic microparticle.[10] To observe unstable (non-self-centering) states, the magnet must be externally constrained to the symmetry axis of the SC ring. Ideally, it could slide down a frictionless fiber. Perhaps the magnetic particle could be slightly charged and held on the axis of a cylindrical capacitor, coinciding with the SC ring axis. Levitation of a magnetic particle, or a high-temperature SC disc with locked-in flux, above a thin type-I superconducting film containing a periodic array of holes is another possible experiment. Such arrays have been fabricated already.[11] As a final suggestion, one could levitate a commensurate array of aligned magnetic dipoles frozen into a nonmagnetic medium. Although the latter system is not analyzed here in detail, it should exhibit behavior similar to the single ring case.

APPENDIX A: LEVITATION OF A MAGNET BY A THICK SC RING

The current flowing around a thick SC ring of wire radius $r \gg \lambda$ is a surface current; thus a contour exists in the bulk of the ring such that $Q=0$. It follows from Eqs. (3.4) and (3.8) that

$$LI = \phi_a + n\phi_0, \tag{A1}$$

where ϕ_a is the applied flux, Eq. (3.6), due to the magnet, enclosed by the contour. Assuming that $h \gg 2r$, the variation of the field in the surface layer around the wire cross section can be neglected and Eq. (3.9) is valid. At equilibrium

$$W = -I\phi_a'. \tag{A2}$$

Eliminating I from Eq. (A1) yields

$$LW + (\phi_a + n\phi_0)\phi_a' = 0. \tag{A3}$$

Equation (A3) determines the temperature-independent states of a magnet levitated, or suspended, by a *thick SC ring* satisfying $\lambda \ll r \ll 0.5h$. Assuming that the flux in a thick ring is conserved, the quantum number is determined by the initial condition $n\phi_0 = LI_0$, where I_0 is the persistent current in the ring prior to the introduction of the magnet.

APPENDIX B: LEVITATION OF A MAGNET BY A SC MICRORING: LONDON APPROXIMATION

In the London theory of superconductivity the current in the SC ring, using the sign convention of Fig. 3(a), is given by

$$I = sj = \frac{s}{\mu_0 \lambda^2(t)} A, \tag{B1}$$

where A is the mean value of the magnitude of the total vector potential over the wire cross section of the ring. Using the integral relation

$$\phi = \oint \mathbf{d}l \cdot \mathbf{A} = 2\pi b A,$$

and $\phi = \phi_a - LI$, the current in Eq. (B1) is

$$I = \frac{\phi_a}{L_0(t) + L}, \quad \text{with } L_0(t) = 2\pi\mu_0 b \frac{\lambda^2(t)}{s}. \tag{B2}$$

Using Eq. (B2) to eliminate I from the equilibrium equation $W=-I\phi_a'$, leads to the self-consistent height equation

$$\frac{4}{3}\mu_0\left(\frac{b^2}{\mu_0 M_0}\right)^2\left[2\left(\frac{\lambda_0}{r}\right)^2\frac{1}{1-t^2}+L'\right]W=\frac{x}{(1+x^2)^4}, \tag{B3}$$

where $x=h/b$, $r=\sqrt{s/\pi}$ is the radius of the wire, and $L'=\ln(8b/r)-1.75$.

With the data used in Sec. III, and with ring radius $b=1$ μm, for example, the ratio $(2/L')(\lambda_0/r)^2=0.49$; thus the London levitation height is temperature dependent. Since the right side of Eq. (B3) has a maximum value of 0.2216 at $x_0=1/\sqrt{7}$ there exists a maximum value of b^4W/M_0^2. Levitation solutions exist for $x>x_0$. For $b=3.345$ μm, the normalized height $x(t)$ is very similar to that shown for $n=0$ in Fig. 4, which is an unstable solution. Increasing the radius of the ring to $b=8$ μm, Eq. (B3) has a strongly temperature-dependent, stable solution $x(t)$ in the range $x(0)=0.7$ to $x(0.85)=0.375$, and the current density remains less than J_c. Increasing b^4W/M_0^2 causes solutions of Eq. (B3) to approach x_0 at lower values of t until finally there is no solution at any temperature. Suspension solutions of Eq. (B3) are not possible in the Meissner state, $n=0$.

Modifying the London Eq. (B1) by the gauge transformation $\mathbf{A}\Rightarrow\mathbf{A}+(\phi_0/2\pi)\nabla\theta$, with the contour integral of $\nabla\theta$ defined to be $2\pi n$, leads to the equation

$$L_0 I=\phi+n\phi_0=\phi_a-LI+n\phi_0, \tag{B4}$$

which is equivalent to $J=Q$, with $J=[\lambda/(\sqrt{2}sH_c)]I$. Equation (B4) follows from Eq. (3.14) in the limit $Q\ll 1$, with Ω neglected. However, note that $J=Q$ does not admit equilibrium solutions for $Q=0$, since J cannot be zero for levitation or suspension. At equilibrium, Eq. (B4) is

$$[L_0(t)+L]W+(\phi_a+n\phi_0)\phi_a'=0. \tag{B5}$$

In contrast to Eq. (B3), Eq. (B5) has suspension solutions for $n<0$. In the limit $L_0(t)\ll L$, Eq. (B5) reduces to the thick ring result, Eq. (A3).

[1] F. C. Moon, *Superconducting Levitation: Application to Bearings and Magnetic Transportation* (Wiley, New York, 1994).

[2] L. C. Davis, E. M. Logothetis, and R. E. Soltis, J. Appl. Phys. **64**, 4212 (1988).

[3] F. Hellman, E. M. Gyorgy, D. W. Johnson, H. M. O'Bryan, and R. C. Sherwood, J. Appl. Phys. **63**,447 (1988).

[4] Z. J. Yang, T. H. Johansen, H. Bratsberg, G. Helgesen, and A. T. Skjeltorp, Physica C **165**, 397 (1990).

[5] S. B. Haley, Phys. Rev. Lett. **74**, 3261 (1995).

[6] D. Shoenberg, *Superconductivity* (Cambridge University Press, Cambridge, England, 1952).

[7] T. P. Orlando and D. A. Delin, *Foundations of Applied Superconductivity* (Addison-Wesley, Reading, MA, 1991), p. 199.

[8] T. Van Duzer and C. W. Turner, *Principles of Superconductive Devices and Circuits* (Elsevier, Amsterdam, 1981), p. 266.

[9] Another choice is to use the experimental values $H_c(0)=0.79\times10^4$ A/m and $\kappa=\lambda(0)/\xi(0)=0.015$ to obtain $\lambda(0)=0.0188$ μm and $\xi(0)=1.25$ μm. This change has no effect on the temperature-independent states, and it only changes the highest "excited" states in Fig. 4. The transition in Fig. 9 occurs for the same value of b and n, but it moves to about $t_{\text{tran}}=0.7$. Since the domain of validity of the GL theory is certainly stretched for $t\ll 1$, it is uncertain which value of $\xi(0)$ is applicable.

[10] G. Weber and K. O. Greulich, Int. Rev. Cytology **133**, 1 (1992); W. H. Wright, G. J. Sonek, and M. W. Berns, Appl. Phys. Lett. **63**, 715 (1993).

[11] A. Bezryadin and B. Pannetier, J. Low Temp. Phys. **98**, 251 (1995); V. V. Moshchalkov *et al.*, Phys. Scr. **T55**, 168 (1994).